Stability of the Modified Euler Method for Nonlinear Dynamic Analysis of TLP

M. R. Tabeshpour[*], A. A. Golafshani, M. S. Seif

[*]Center of Excellence in Hydrodynamics and Dynamics of Marine Vehicles, Mechanical Engineering Department, Sharif University of Technology, Tehran, Iran; tabeshpour@sharif.edu

ARTICLE INFO

ABSTRACT

Efficiency of numerical methods is an important problem in dynamic nonlinear analyses. It is possible to use of numerical methods such as beta-Newmark in order to investigate the structural response behavior of the dynamic systems under random sea wave loads but because of necessity to analysis the offshore systems for extensive time to fatigue study it is important to use of simple stable methods for numerical integration. The modified Euler method (MEM) is a simple numerical procedure which can be effectively used for the analysis of the dynamic response of structures in time domain. It is also very effective for response dependent systems in the field of offshore engineering. An important point is investigating the convergence and stability of the method for strongly nonlinear dynamic systems when high initial values for differential equation or large time steps are considered for numerical integrating especially when some frequencies of the system is very high. In this paper the stability of the method for solving differential equation of motion of a nonlinear offshore system (tension leg platform, TLP) under random wave excitation is presented. In this paper the stability criterion and the convergence of the numerical solution for critical time steps are presented.

1. Introduction

Many studies have been carried out to understand the structural behavior of TLP and determine the effect of several parameters on dynamic response and average life time of the structure [1–6]. The tether system is a critical and basic component of the TLP. The most important point in the design of TLP is the pretension of the legs. The pretension causes that the platform behaves like a stiff structure with respect to the vertical degrees of freedom (heave, pitch and roll), whereas with respect to the horizontal degrees of freedom (surge, sway and yaw) it behaves as a floating. structure. Therefore the periods of the vertical degrees of freedom are lower than the others. Another important problem is investigating the effects of radiation and scattering on the hull and tendon responses. An analytical solution for surge motion of TLP was proposed and demonstrated [7], in which the surge motion of a platform with pre-tensioned tethers was calculated. In that study, however, the elasticity of tethers was only implied and the motion of tethers was also simplified as on-line rigid-body motion proportional to the top platform. Thus, both the

material property and the mechanical behavior for the tether incorporated in the TLP system were ignored. When this simplification was applied, no matter what the material used was or what the dimension of tethers was, the dynamic response of the platform would remain the same in terms of the vibration mode, periods and the vibration amplitude. An important point in that study was linearization of the surge motion. But it is obvious that the structural behavior in the surge motion is highly nonlinear because of large deformation of TLP in the surge motion degree of freedom (geometric nonlinearity) and nonlinear drag forces of Morison equation. Therefore the obtained solution is not true for the actual engineering application. For heave degree of freedom the structural behavior is linear, because there is no geometric nonlinearity in the heave motion degree of freedom and drag forces on legs have no vertical component. Similarly, an analytical heave vibration of TLP with radiation and scattering effects for damped systems

has been presented [8]. a similar method is presented for hydrodynamic pitch response of the structure [9]. The modified Euler method [10] presented herein is a

simple numerical procedure which can be effectively used for the analysis of the dynamic response of structures in the time domain. It has been shown that the modified Euler method is conditionally stable [11]. The application of the modified Euler method made herein shows that it is efficient and easy to use, and that it can be employed to obtain accurate solutions to a wide variety of structural dynamics problems. Simplicity is one of the distinguishing features of the method. Because the modified Euler method is conditionally stable, it may be inefficient for the analysis by direct integration of the response of a multidegree-of-freedom system with a very short highest natural period of vibration. However, the method is explicit, and it is particularly sited for the analysis of non-linear systems. The modified Euler method has been successfully used in the analysis for the dynamic response of wave-excited offshore structures [12].

A Comprehensive study on the results of tension leg platform responses in random sea considering all structural and excitation nonlinearities is presented by Tabeshpour et al. [13]. This kind of interpretation of the results is necessary for optimum design of TLP. The effect of added mass fluctuation on the pitch response of tension leg platform has been investigated by using perturbation method both for discrete and continues models [14]. Liu et al. described an analysis of the non-linear effects and identification of non-linear pitch motion on tension leg platforms. The purpose of their paper was to accurately identify pitch motion on the tension leg platform and to interpret the non-linear effects using statistical methods, the NARMAX methodology, and the higher order frequency response functions [15].

Chandrasekaran et al. investigated the response of triangular tension leg platform (TLP) for different wave approach angles varying from 0° through 90° and its influence on the coupled dynamic response of triangular TLPs [16]. Barranco-Cicilia et al. presented a methodology to perform a Load and Resistance Factor Design (LRFD) criterion for the design of tension leg platforms (TLP) tendons in their intact condition [17]. A robust stochastic design framework were discussed for design of mass dampers by Taflanidis et al. The focus was on applications for the mitigation of the coupled heave and pitch response of Tension Leg Platforms under stochastic sea excitation [18].

Tabeshpour et al. investigated design and effect of tuned mass damper on response of tension leg platform under wind and wave forces [19]. Efficiency of numerical methods is an important problem in dynamic nonlinear analyses. It is possible to use of numerical methods such as beta-Newmark in order to investigate the structural response behavior of the dynamic systems under random sea wave loads but because of necessity to analysis the offshore systems

for extensive time to fatigue study it is important to use of simple stable methods for numerical integration. The key point of suitability of MEM for solving the TLP system is that the maximum frequency of the system is about 0.5 Hz. In this paper the convergence and stability of the method for solving differential equation of motion of a nonlinear offshore system known as tension leg platform under random wave excitation is presented.

2. The Modified Euler Method (Mem)

Consider the numerical evaluation of the free-vibrational response of a linear, undamped, simple mass-spring system governed by the following differential equation:

$$\ddot{x} + \omega^2 x = 0 \tag{1}$$

in which x is the displacement of the system; ω is the circular natural frequency of vibration of the system; and a dot superscript denotes differentiation with respect to time, t. Let x_n and $\dot{x}_n$ be the known displacement and velocity, respectively, of the system at time t_n. This time is expressed in terms of a non-negative integer number, n, and a time step, Δt, as $t_n = n\Delta t$. By application of the MEM, the displacement and velocity of the system, x_{n+1} and $\dot{x}_{n+1}$, at time $t_{n+1} = (n+1)\Delta t$, are evaluated as follows. By using eq. (1), compute

$$\ddot{x}_n = -\omega^2 x_n \tag{2}$$

Then, compute

$$\dot{x}_{n+1} = \dot{x}_n + \ddot{x}_n \Delta t \tag{3}$$

Now there is two approaches in order to calculate $\dot{x}_{n+1}$. First approach is using only the velocity in time step $n+1$:

$$x_{n+1} = x_n + \dot{x}_{n+1} \Delta t \tag{4}$$

The second one is averaging of velocities of two steps:

$$x_{n+1} = x_n + \frac{\dot{x}_{n+1} + \dot{x}_n}{2} \Delta t \tag{5}$$

If one uses the following equation

$$x_{n+1} = x_n + \dot{x}_n \Delta t \tag{6}$$

then the method is called Euler method. With the values of x_{n+1} and $\dot{x}_{n+1}$ available, the procedure defined by eqs. (2)-(4 or 5) may be repeated to compute the response of the system for subsequent discrete times larger than t_{n+1}. These computations can be carried out accurately by a proper

implementation of the MEM. It is important to note that, in the MEM, the solution for x_{n+1} is based on using the equilibrium equation at time t_n. Therefore, the MEM is an explicit method. It is also important to note in eq. (4) that the displacement x_{n+1} is computed by using the velocity $\dot{x}_{n+1}$. If $\dot{x}_{n+1}$ is replaced in eq. (4) with $\dot{x}_n$, then the procedure defined by eqs. (2)-(4) reduces to the well known standard Euler method, which is an unstable approach that should never be used for structural dynamics applications.

3. Stability Analysis for the Mem

Eq. (2) is substituted into eq. (3), and eq. (4) is rewritten to obtain

$$\dot{x}_{n+1} = \dot{x}_n - \Delta t\, \omega^2 x_n \qquad (7)$$

$$x_{n+1} = x_n + \Delta t\, \dot{x}_{n+1} \qquad (8)$$

and it is apparent from eqs. (14) and (15) that

$$\dot{x}_n = \dot{x}_{n-1} - \Delta t\, \omega^2 x_{n-1} \qquad (9)$$

$$x_n = x_{n-1} + \Delta t\, \dot{x}_n \qquad (10)$$

Subtracting eq. (10) from eq. (8) leads to

$$x_{n+1} - x_n = x_n - x_{n-1} + \Delta t\, (\dot{x}_{n+1} - \dot{x}_n) \qquad (11)$$

and the quantity $(\dot{x}_{n+1} - \dot{x}_n)$ may be obtained from eq. (3) and substituted into eq. (18) to obtain

$$x_{n+1} - (2 - \Delta t^2 \omega^2) x_n + x_{n-1} = 0 \qquad (12)$$

Eq. (19) is a linear homogeneous difference equation of second order (Karman and Biot, 1940) and it can be rewritten as

$$x_{n+2} - (2 - \Delta t^2 \omega^2) x_{n+1} + x_n = 0 \qquad (13)$$

the solution of which may be expressed as

$$x_n = \lambda^n \qquad (14)$$

By substituting eq. (14) into eq. (13), the following characteristic equation is obtained:

$$\lambda^2 - (2 - \Delta t^2 \omega^2)\lambda + 1 = 0 \qquad (15)$$

and the roots of eq. (15), λ_1 and λ_2, provide the values of λ which are needed to find x_n in accordance with eq. (14). These roots are found to be

$$\lambda_1 = (1 - 0.5\Delta t^2 \omega^2) + 0.5\Delta t\, \omega(\Delta t^2 \omega^2 - 4)^{1/2} \quad (16)$$

$$\lambda_2 = (1 - 0.5\Delta t^2 \omega^2) - 0.5\Delta t\, \omega(\Delta t^2 \omega^2 - 4)^{1/2} \qquad (17)$$

There are three important cases: in Case 1, the roots are real-valued and distinct; in Case 2, the roots are real-valued and equal; and in Case 3, the roots are

complex-valued quantities. Cases 1 and 2 lead to unstable solutions for x_n; and Case 3, which leads to stable solutions, is obtained if

$$\Delta t^2 \omega^2 < 4 \qquad (18)$$

This expression gives the condition for the stability of the MEM and may be reformulated as

$$\Delta t < \frac{T}{\pi} \qquad (19)$$

in which $T = 2\pi / \omega$ is the natural period of vibration of the system. Therefore, the MEM is stable only when eq. (26) is satisfied.

Similar calculation and considering eq. (12) instead of (11) results in

$$\Delta t < \frac{2T}{\pi} \qquad (20)$$

Assuming that the condition for stability is satisfied, eqs. (16) and (17) may be rewritten as

$$\lambda_1 = (1 - 0.5\Delta t^2 \omega^2) + i\, 0.5\Delta t\, \omega(4 - \Delta t^2 \omega^2)^{1/2} = e^{i\mu} \quad (21)$$

$$\lambda_2 = (1 - 0.5\Delta t^2 \omega^2) - i\, 0.5\Delta t\, \omega(4 - \Delta t^2 \omega^2)^{1/2} = e^{-i\mu} \quad (22)$$

where $i = \sqrt{-1}$, and

$$\mu = \arctan\left(\frac{0.5\Delta t\, \omega(4 - \Delta t^2 \omega^2)^{1/2}}{1 - 0.5\Delta t^2 \omega^2}\right) \qquad (23)$$

and the solution for the displacements x_n is obtained from eqs. (14), (20) and (21) as

$$x_n = C_1 e^{in\mu} + C_2 e^{-in\mu} \qquad (24)$$

or, alternatively, as

$$x_n = D_1 \cos(n\eta) + D_2 \sin(n\eta) \qquad (25)$$

in which C_1, C_2, D_1 and D_2 are constants to be determined from the specified initial conditions.

4. TLP, Strongly Nonlinear System

Because of large displacement of TLP and nonlinear terms in exciting force, the equation of motion of TLP is strongly nonlinear and the exciting wave force is response dependent as well (Chandrasekaran, S., Jain, A.K., 2001, 2002). A brief review on structural modeling of TLP is presented here in.

5. Mass Matrix of TLP

Structural mass is assumed to be lumped at each degree of freedom. Hence, it is diagonal in nature and is constant. The added mass, M_a, due to the water surrounding the structural members and arising from the modified Morrison equation is considered up to

the mean sea level (MSL) only. The fluctuating component of added mass due to the variable submergence of the structure in water is considered in the force vector depending upon whether the sea surface elevation is above (or) below the MSL. The mass matrix of TLP is

$$[M] = \begin{array}{c} |Surge \quad Sway \quad Heave \quad Roll \quad Pitch \quad Yaw| \\ \begin{bmatrix} M'_{SS} & 0 & 0 & 0 & 0 & 0 \\ 0 & M'_{WW} & 0 & 0 & 0 & 0 \\ 0 & 0 & M'_{HH} & 0 & 0 & 0 \\ M_{aRS} & M_{aRW} & M_{aRH} & M_{RR} & 0 & 0 \\ M_{aPS} & M_{aPW} & M_{aPH} & 0 & M_{PP} & 0 \\ 0 & 0 & 0 & 0 & 0 & M_{YY} \end{bmatrix} \end{array}$$

(26)

where $M_{SS} = M_{WW} = M_{HH} = M$ and $M'_{SS} = M_{SS} + M_{aSS}$ and $M'_{WW} = M_{WW} + M_{aWW}$ and $M'_{HH} = M_{HH} + M_{aHH}$. M is the total mass of the entire structure, M_{RR} is the total mass moment of inertia about the x axis = Mr_x^2, M_{PP} is the total mass moment of inertia about the y axis = Mr_y^2, M_{YY} is the total mass moment of inertia about the z axis = Mr_z^2, r_x is the radius of gyration about the x axis, r_y is the radius of gyration about the y axis, and r_z is the radius of gyration about the z axis. The added mass terms are:

$$M_{aSS} = M_{aWW} = M_{aHH} = 0.25\pi D^2 (C_m - 1)\rho dl \quad (27)$$

$$M_{aSS} = \int_{lenght} dM_{aSS} \quad (28)$$

M_{aRS} is the added mass moment of inertia in the roll degree of freedom due to hydrodynamic force in the surge direction. M_{aRW} is the added mass moment of inertia in the roll degree of freedom due to hydrodynamic force in the sway direction. M_{aRH} is the added mass in the roll degree of freedom due to hydrodynamic force in the heave direction. M_{aPS} is the added mass moment of inertia in the pitch degree of freedom due to hydrodynamic force in the surge direction. M_{aPW} is the added mass moment of inertia in the pitch degree of freedom due to hydrodynamic force in the sway direction. M_{aPH} is the added mass in the pitch degree of freedom due to hydrodynamic force in the heave direction. The presence of off diagonal terms in the mass matrix indicates a contribution in the added mass due to the hydrodynamic loading. The loading will be attracted only in the surge, heave and pitch degrees of freedom due to the unidirectional wave acting in the surge

direction on a symmetric configuration of the platform about the *x* and *z* axes).

6. Stiffness Matrix of the TLP

The coefficients, K_{AB}, of the stiffness matrix of the triangular TLP are derived as the reaction in the degree of freedom *A* due to unit displacement in the degree of freedom *B*, keeping all other degrees of freedom restrained. The coefficients of the stiffness matrix have nonlinear terms due to the cosine, sine, square root and squared terms of the displacements. Furthermore, the tendon tension changes due to the motion of the TLP in different degrees of freedom makes the stiffness matrix response-dependent. The stiffness matrix [*K*] of a TLP is:

$$[K] = \begin{array}{c} |Surge \quad Sway \quad Heave \quad Roll \quad Pitch \quad Yaw| \\ \begin{bmatrix} K_{SS} & 0 & 0 & 0 & 0 & 0 \\ 0 & K_{WW} & 0 & 0 & 0 & 0 \\ K_{HS} & K_{HW} & K_{HH} & K_{HR} & K_{HP} & K_{HY} \\ 0 & K_{RW} & 0 & K_{RR} & 0 & 0 \\ K_{PS} & 0 & 0 & 0 & K_{PP} & 0 \\ 0 & 0 & 0 & 0 & 0 & K_{YY} \end{bmatrix} \end{array}$$

(29)

In the stiffness matrix the presence of off-diagonal terms, reflects the coupling effect between the various degrees of freedom and the coefficients depend on the change in the tension of the tendons, which is affecting the buoyancy of the system. Hence, the [*K*] is not constant for all time instants but the coefficients are replaced by a new value computed at each time instant depending upon the response value at that time instant. The stiffness matrix of the four-legged square TLP is taken as suggested by Morgan and Malaeb (1983).

7. Damping Matrix, [C]

Assuming [*C*] to be proportional to [*K*] and [*M*], the elements of [*C*] are determined by the equation given below, using the orthogonal properties of [*M*] and [*K*]:

$$C = \alpha M + \beta K \quad (30)$$

α and β are constant. This matrix is calculated based on the initial values of [*K*] and [*M*] only.

8. Wave Forces

The problem of suitable representation of the wave environment or more precisely the wave loading is the problem of prime concern. Once the wave environment is evaluated, wave loading on the structure may be computed based on suitable theory. In this work the water particle position η is determined according to Airy's linear wave theory:

$$\eta(x,t) = A\cos(kx - \omega t) \quad (31)$$

where A is the amplitude of the wave, k is the wave number, ω is the wave frequency and x is the horizontal distance from the origin.

In stochastic modeling, sea waves are commonly characterized by their PSDFs. Water particle kinematics, at different location on the structure, are considered to be derived processes and these need not be specified in addition to the sea surface elevation. On account of various physical processes involved in the generation of waves, a random wave is regarded as a superposition of an infinite number of independent waves of different wave heights and wave periods with arbitrary phase angles. In the present simulation procedure, waves are assumed to be stationary, homogeneous and ergodic in the statistical sense. By considering the random process as a linear superposition of a large number of independent waves, its distribution becomes Gaussian. Depending upon the fetch conditions, several analytical expressions exist for the approximation of the sea surface elevation spectrum (i.e. its PSDF). A well-known spectrum model for ocean waves is Peirson-Moskowitz (P-M) model. The modified P-M spectrum model is assumed to adequately represent the sea state. It is given by:

$$S_{\eta\eta}(\omega) = \frac{H_s^2 T_z}{8\pi^2} \left\{ \frac{T_z \omega}{2\pi} \right\}^{-5} \exp\left\{ -\frac{1}{\pi}\left(\frac{T_z \omega}{2\pi} \right)^{-4} \right\} \quad (32)$$

where H_s is the significant wave height in m, T_z is zero up crossing period in s and ω is the angular frequency. Figure 1 shows the curve of the spectrum.

The linearized small-amplitude wave theory allows the summation of velocity potential, wave elevation, and water particle kinematics of the individual regular wave to form a random wave made up of a number of components. The generated synthetic random wave is considered to be adequately represented by a summation of linear harmonic regular waves. The series representation of sea surface elevation is given by the equation

$$\eta(x,t) = \lim \sum_{i=1}^{k} A_i \cos(k_i x - \omega_i t + \varphi_i) \quad (33)$$

$$A_i = \sqrt{2 S_{\eta\eta}(\omega_i) \Delta \omega_i} \quad (34)$$

where A_i is the amplitude of the i-th component wave, k_i is the wave number of the i-th component wave, ω_i is the wave frequency of the i-th component wave, φ is the phase angle of the i-th component wave, varying between 0 and 2π, x is the horizontal distance from the origin and $S_{\eta\eta}(\omega)$ is the one-sided sea surface elevation PSDF. Once the sea surface elevation time history $\eta(x,t)$ is known from Eq. (33), the time

histories of the water particle velocity and acceleration are computed by wave superposition, according to Airy's linear wave theory. The horizontal water particle velocity $\dot{u}(x,t)$ and the vertical water particle velocity $\dot{v}(x,t)$ are given as:

$$\dot{u}(x,t) = \sum_{i=1}^{k} A_i \omega_i \cos(k_i x - \omega_i t + \varphi_i) \frac{\cosh(k_i z)}{\sinh(k_i(d+\eta))} \quad (35)$$

$$\dot{v}(x,t) = \sum_{i=1}^{k} A_i \omega_i \sin(k_i x - \omega_i t + \varphi_i) \frac{\sinh(k_i z)}{\sinh(k_i(d+\eta))} \quad (36)$$

where k_i is the i-th component wave number, y is the vertical distance at which the wave kinematics is calculated, d is the water depth, η is the sea surface elevation, which is equal to $\eta(x,t)$ given by Eq. (31). The wave forces acting on the cylindrical member of the TLP structure are obtained by using modified Morison's equation, which takes relative velocity and acceleration between the structure and water particles into account. While calculating the wave forces, water particle kinematics for each member are determined with respect to the average value across the diameter of the member. The integration of the elemental forces acting on the pontoons and columns is performed numerically by dividing the cylinder into small elements. The instantaneous total hydrodynamic force is determined at each time station with the assigned values of the structural displacements, velocities and accelerations.

In order to probability work on the wave height the knowledge of the wave height distribution is of great importance since various valuable information can be derived from this distribution. It has been found that wave heights of an irregular sea follow a Rayleigh distribution.

9. Hydrodynamic Force

Water particle kinematics are evaluated using Airy's linear wave theory. This description assumes the wave form whose wave height, H, is small in comparison to its wave length, L, and water depth, d. Knowing the water particle kinematics, the hydrodynamic force vector is calculated in each degree of freedom. According to Morison's equation, the intensity of wave force per unit length on the structure is given as:

$$f(x,y,t) = 0.5\rho_w C_d D(\dot{u} - \dot{x} + \dot{u}_c)|\dot{u} - \dot{x} + \dot{u}_c| + 0.25\pi D^2 \rho_w C_m \ddot{u} \pm \left(0.25\pi D^2 [C_m - 1]\rho_w \ddot{x}\right) \quad (37)$$

where $\dot{u}_c$ is the current velocity, $\dot{u}$ is the horizontal water particle velocity, $\dot{x}$ is the horizontal structural velocity, D is the diameter of the column, $\ddot{x}$ is the horizontal structural acceleration, and $\ddot{u}$ is the

horizontal water particle acceleration. The last term in Eq. (37) is the added mass term and a positive sign is used when the water surface is below the MSL and a negative sign is used when water surface is above the MSL. The contribution of added mass up to the MSL will already be considered along with structural mass. It is seen that both structural stiffness and external load are nonlinear.

10. Equation of Motion

The equation of motion of the TLP under a regular wave is given as:

$$[M]\{\ddot{X}\} + [C]\{\dot{X}\} + [K]\{X\} = \{F(t)\} \tag{38}$$

where $[M], [C]$ and $[K]$ are the matrices of mass, damping and stiffness respectively, $\{X\}$, $\{\dot{X}\}$ and $\{\ddot{X}\}$ are the structural displacement, velocity and acceleration vector respectively and $\{F(t)\}$ is the excitation force vector.

11. Suitability of Mem for TLP Analysis

The most important reason of suitability of MEM for solving the differential equation of motion of TLP is that the natural periods of TLP are limited between 1.5 sec to 120 sec and therefore the criterion of being small time step is easily satisfied. In order to satisfy the stability condition developed in eq. (19) for systems with multiple degrees of freedom the time step should satisfy the equation $\Delta t < T_{min} / \pi$ in which T_{min} is the lowest period of the system. Minimum natural period of TLP is related to one of the stiff degrees of freedom: heave, roll or pitch. This value is abot 1.5 to 2.5 sec. Therefore considering $\Delta t < 1.5 / \pi$ the solution will be stable.

12. Numerical Study

A TLP in 500 *m* deep water has been chosen for the numerical study. The characteristics of the TLP under study are: Diameter of Column $D_c = 18m$; Diameter of Pontoon $D = 12m$ and hull length is $80m$. Tether tensions are assumed to be equally distributed in all the four tethers. TLP structure is assumed to behave like a rigid body. The stiffness matrix developed takes into account large deformations and other nonlinearities like tether tension, etc. The angle of attack of long crested sea is $30°$ with *x* direction and $H_s = 10$ *m* , $T_z = 15$ sec . Figure (1) shows the spectrum of sea-state for $H_s = 10$ *m and* $T_z = 15$ sec . Based on the mentioned formulation, random surface elevation has been derived. A typical generated wave is shown in Figure 2.

Eigenvalue analysis results the following periods: Surge: 72.8 sec; Sway: 72.8 sec ; Heave: 2.44 sec; Roll: 2.16 sec; Pitch: 2.16 sec; and Yaw: 87.8 sec. A computer program (SNATELP) has been developed

using MATLAB, for nonlinear dynamic analysis of TLP system.

The minimum period of the structure is related to roll and pitch motion. Cosidering eq. (19) in order to satisfy the stability condition, time step should be $\Delta t < 2.16 / \pi = 0.68$ sec . It means that if one considers $\Delta t = 0.67$ sec ($\Delta t - \varepsilon$) the solution will be stable and for $\Delta t = 0.69$ sec ($\Delta t + \varepsilon$) it is not stable. ε is a small variation in time step.

Time history of deformations is illustrated in figure 3 for $\Delta t = 0.67$ sec . In order to have a better view on the responses they are plotted in time between 200 to 500 sec and 400 to 500 sec in figures 4 and 5. It is seen that the solution is stable and has converged to the steady state response related to wave excitation and structural period. For stiff degrees of fredom (heave, roll, pitch) the stable converged response is seen clearly after about 100 seconds. But for flexible degrees of freedom (surge, sway, yaw) from the beginning of the motion, stable response is viewed. Phase planes are useful to interpret the stability of motion fand gives a conceptual view of structural response. Phase planes of all degrees of freedom are plotted in Figure 6. It is seen that all rsponses are limited to the higher bound of deformation and related velocity. Dense graphs of phase plane for stiff degrees of fredom shows that we are near the boundary of stability.

Similar plots for $\Delta t = 0.68$ sec are illustrated in figures 7-10. It is clearly observed beating phenomenon in both roll and pitch motions because of small difference between roll period rounded to 0.68 sec and considered time step. It means that $\Delta t = 0.68$ sec is the boundary limit of time step to lead to stable solution or not. In figure 9 it is seen the resonance type motion of roll and pitch motions. Phase plane of these motions shown in figure 10 represents the resonance type motion and no stability point.

It is noted that beating type response of roll and pitch is related to the marginal instability condition. If only a small increasing occurs in Δt them the clear instability will be seen. In order to have a view on the instability of solutions similar plots are illustrated for $\Delta t = 0.69$ sec in figures 11-14. It is seen that roll and pitch responses have a large amplitude of vibration with a constant period of motion.

There is no convergence and stability in roll and pitch motions. Figure 11 shows that pitch and roll motions have large amplitudes with no convergence. Also there is no stability point for pitch and roll in figure 14.

Now Δt is increased to 0.7 sec. Similar plots for $\Delta t = 0.7$ sec are illustrated in figures 15-18. Comparing the amplitude of roll and pitch sown in Figure 13 with Figure 17, one can find that increase in time step of integration leads to increase in amplitude of unstable response. Also there is relatively linear

relation between rotation and velocity both for roll and pitch motion.

As mentioned above the period of heave motion is equal to 2.44 sec. However the response of heave motion is stable for all values of discussed Δt, but for $\Delta t = 2.44 / \pi = 0.78$ sec the heave response is not converged to a finite value and the amplitude of vibration increases rapidly at the start of the motion as shown in figures 19 and 20.

After $t = \Delta t$ (at the end of first step) High amplitude motions of stiff degrees of freedom is observed. Note that after 4 sec the amplitude of heave motions is more than surge motion. The structural periods of surge, sway and yaw motions are very high. But for stiff degrees of freedom (roll, pitch and heave) that their period is about 1.5 to 2.5 sec it is important to have a view on stability condition. Also however the system is coupled, it can be separately investigated the condition of stability for each degree of freedom as mentioned in the text

13. Conclusion

The convergence and stability of the MEM for strongly nonlinear dynamic system (TLP) under random wave excitation was discussed. The key point of suitability of the MEM for solving the TLP system is that the maximum frequency of the system is less than 0.5Hz. However the MEM is conditionally stable, it is very efficient for solving response dependent offshore systems with bounded maximum natural frequency. The importance of using such simple methods with relatively large time step is on the fatigue study and necessity to develop time history of responses for long time. Based on the numerical example it can be said that it is possible using the MEM for TLP system with large time step for integration. This leads to consuming in time and ability of doing complicated nonlinear dynamic analyses in design process.

14. References

1- Faltinsen, O.M., Van Hooff, R.W., Fylling, I.J. and Teigen, P.S., (1982), *Theoretical and experimental investigations of tension leg platform behavior*, In: Proceedings of BOSS 1, p.411–23.

2- Siddiqui, N.A. and Ahmad, S., (2001), *Fatigue and fracture reliability of TLP tethers under random loading*, Marine Structures, Vol.14, p.331–52.

3- Teigen PS., (1983), *The response of a tension leg platform in short-crested waves*, In: Proceedings of the offshore technology conference, OTC No. 4642, p. 525–32.

4- Jain A.K. (1997), *Nonlinear coupled response of offshore tension leg platforms to regular wave forces*, Ocean Eng., Vol.24(7), p.577–92.

5- Ahmad, S., (1996), *Stochastic TLP response under long crested random sea*, J Comp Struct, Vol.61(6), p.975–93.

6- Chandrasekaran S, Jain AK. (2002), *Triangular configuration tension leg platform behavior under random sea wave loads*, Ocean Eng., Vol. 29(15), p.1895–1928.

7- Lee HH, Wang P-W and Lee C-P. (1999), *Dragged surge motion of tension leg platforms and strained elastic tethers*, Ocean Eng., Vol.26(2), p.579–94.

8- Tabeshpour M.R., Golafshani A.A., Ataie Ashtiani B., Seif M.S., (2006), *Analytical solution of heave vibration of tension leg platform*, Int J Hydrol Hydromechanics Vol. 54(3) p.280–288.

9- Tabeshpour M.R., Ataie Ashtiani B., Seif M.S. and Golafshani A.A., (2006), *Wave interaction pitch response of tension leg structures*, In: 13th international congress on sound and vibration, Austria, Vienna.

10- Karman, T. V. and Biot, M. A., (1940)., *Mathematical in Engineering*, McGraw-Hill, NewYork.

11- Hahn, G.D., (1990), *A Modified Euler method for dynamic analysis*, International Journal for Numerical Methods in Engineering, Vol. 32, No 3, p. 943-955.

12- Sanghvi, JR, (1990), *Simplified dynamic analysis of offshore structures*, M.S. Thesis, Department of Civil and Environmental Engineering, Vanderbilt University.

13- Tabeshpour, M. R., Golafshani, A. A. and Seif, M. S., (2006*), A Comprehensive study on the results of tension leg platform responses in random sea*, Journal of Zhejiang University, Vol. 7, No. 8, p. 1305-1317.

14- Tabeshpour, M.R., Golafshani, A.A. and Seif, M.S., (2006a), *Second order perturbation added mass fluctuation on vertical vibration of TLP*, Marine Structures, Vol.19 (4), p.271–283.

15- Liu, J., Huang ,Y. and Lin, H., (2004), *Nonlinear pitch motion identification and interpretation of a tension leg platform*, Journal of Marine Science and Technology, Vol. 12, No. 4, p. 309-318.

16- Chandrasekaran, S., Jain, A.K. and Gupta, A., (2007), *Influence of wave approach angle on TLP's response*, Ocean Engineering, Vol. 34, Issues 8-9, p.1322-1327.

17- . Barranco-Cicilia, F, Lima, E.C.P., Sagrilo, L.V.S., (2008), *Reliability-based design criterion for TLP tendons, Applied Ocean Research*, Vol. 30, Issue 1, p. 54-61.

18- Taflanidis, A.A., Angelides, D.C. and Scruggs, J.T., (2009), *Simulation-based robust design of mass dampers for response mitigation of tension leg platforms, Engineering Structures*, Vol. 31, Issue 4, p. 847-857.

19- Tabeshpour, M.R., dehkharghanian, V., and Dovlatshahi, M., (2010), *The effect of tuned mass damper on vertical vibration of TLP*, 12th National marine industrial conference.
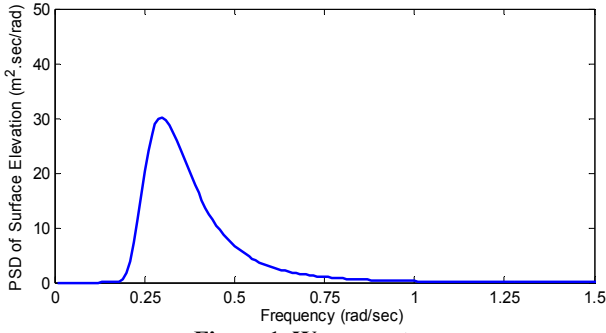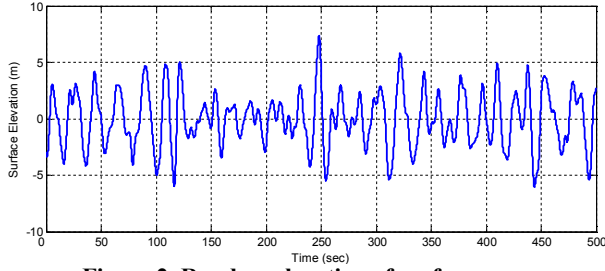
Figure 1. Wave spectrum

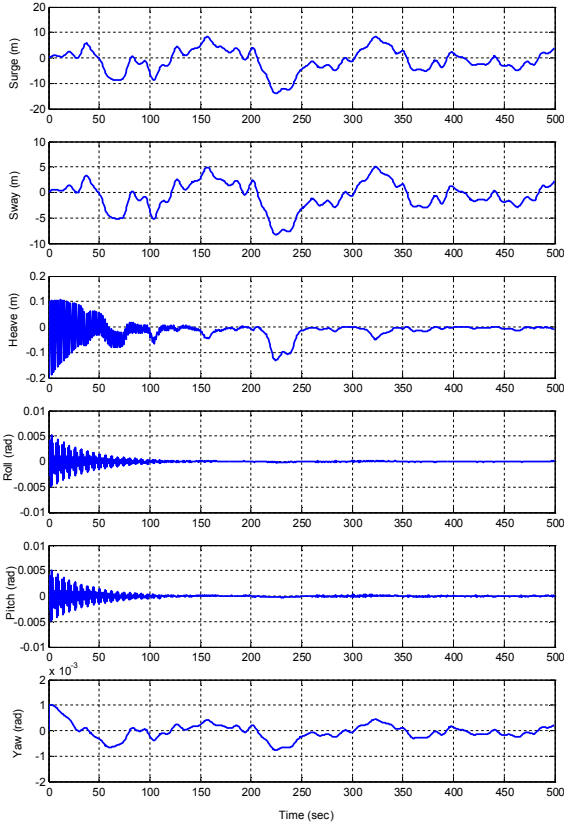**Figure 2. Random elevation of surface wave**

Figure 3. Time history of deformations, $\Delta t = 0.67\,\text{sec}$
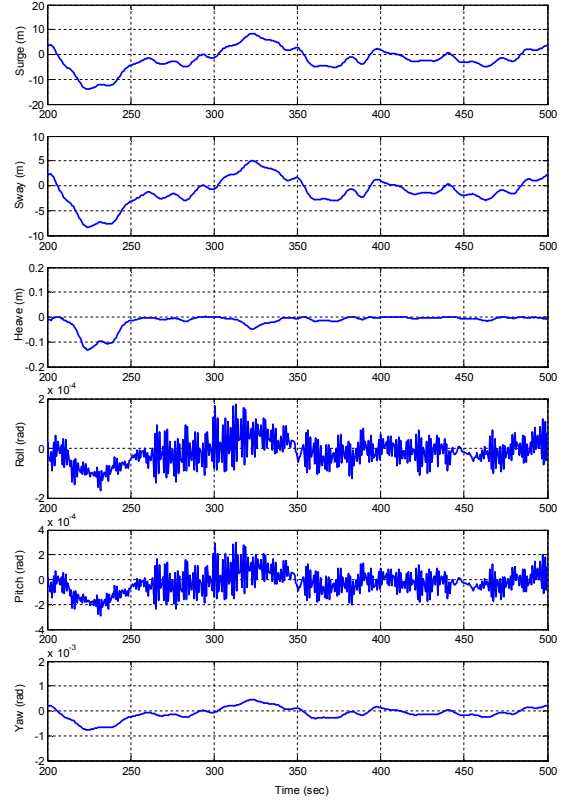

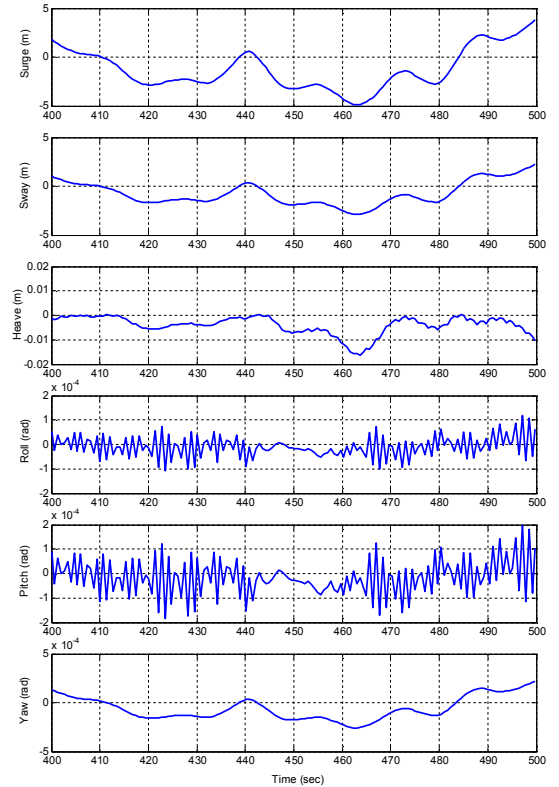**Figure 4. Time history of deformations in time between 200-500 sec, $\Delta t = 0.67\,\text{sec}$**

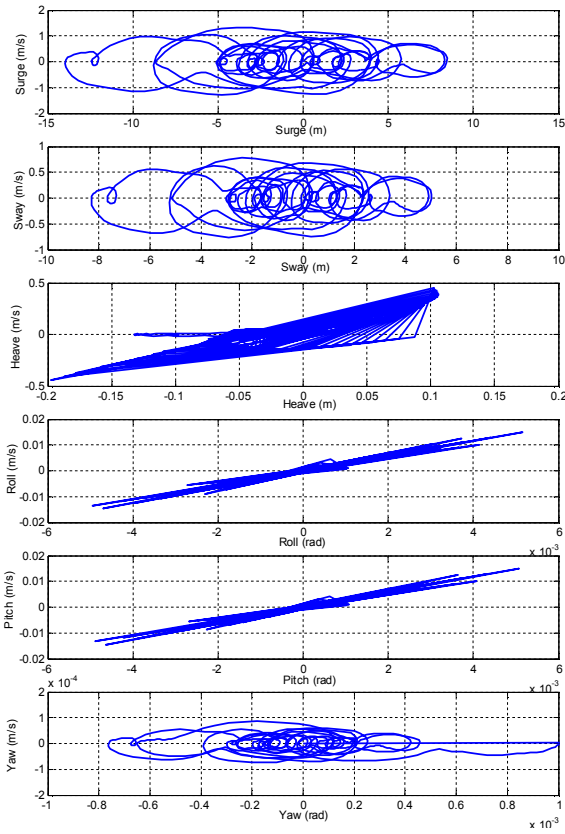**Figure 5. Time history of deformations in time between 400-500 sec, $\Delta t = 0.67\,\text{sec}$**
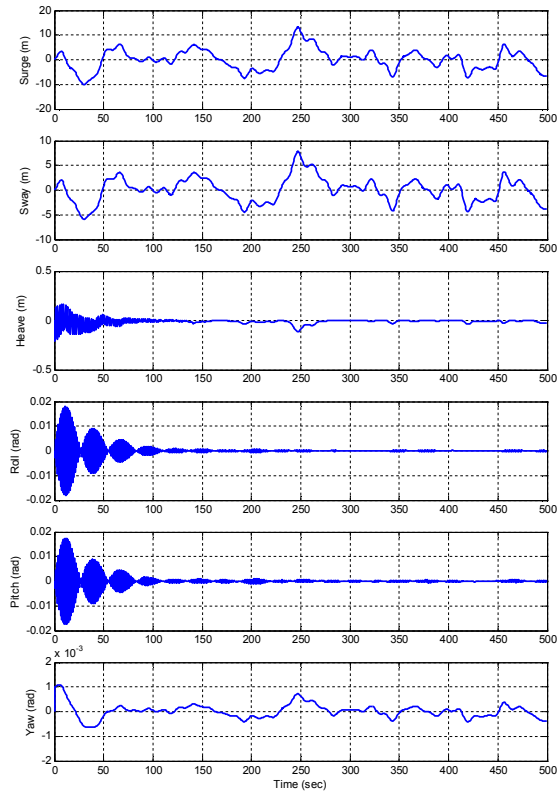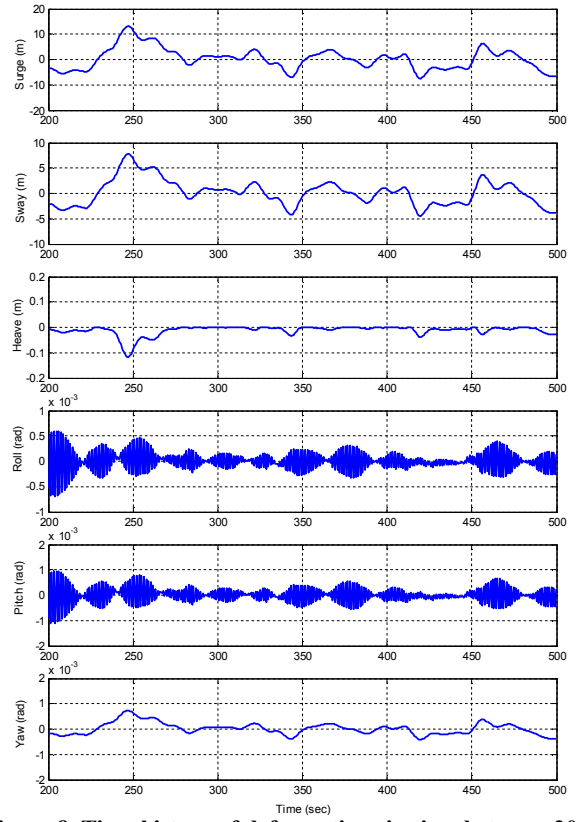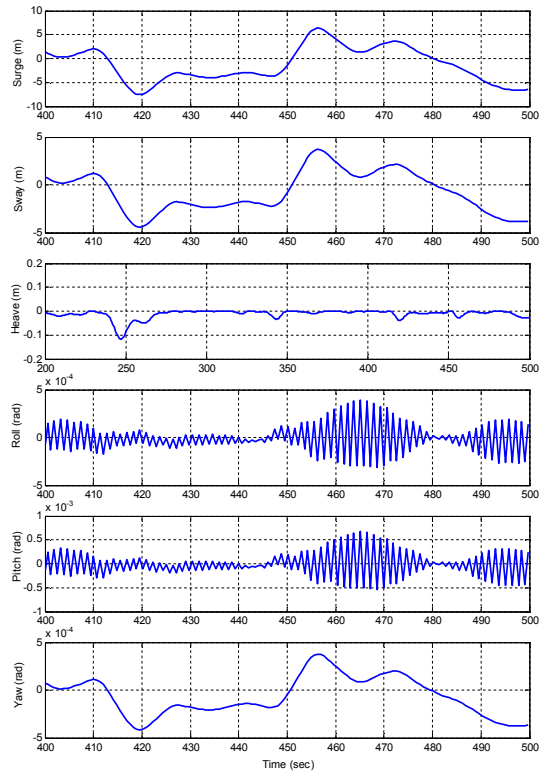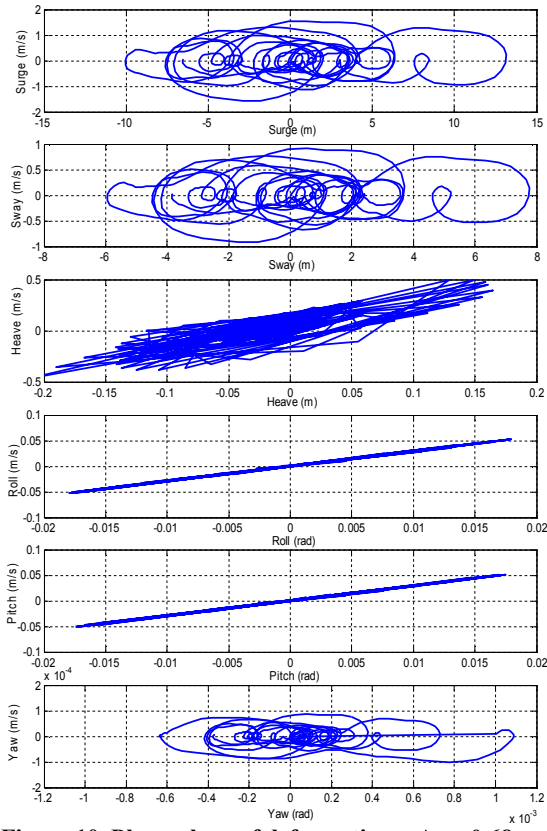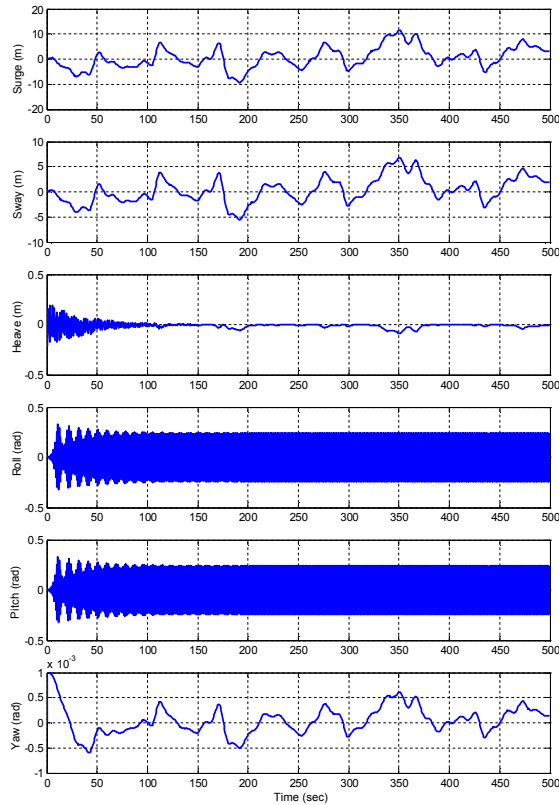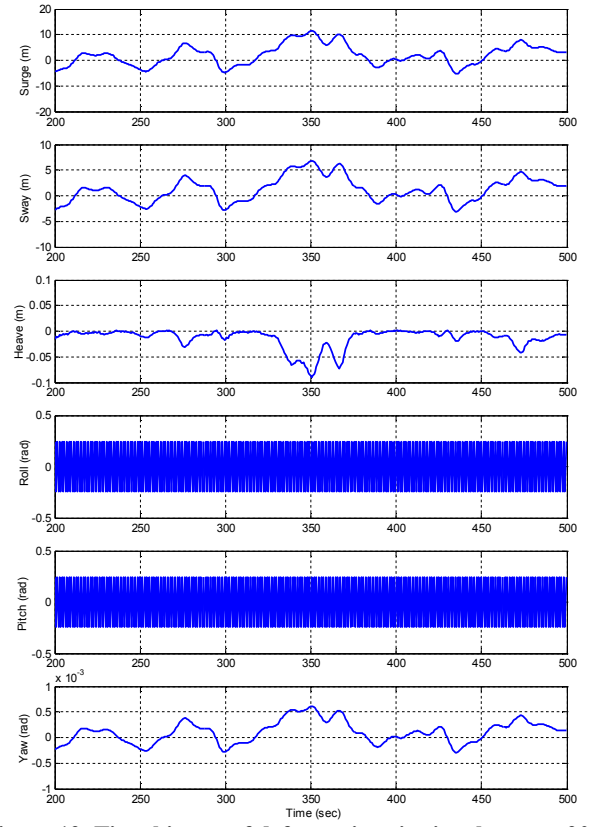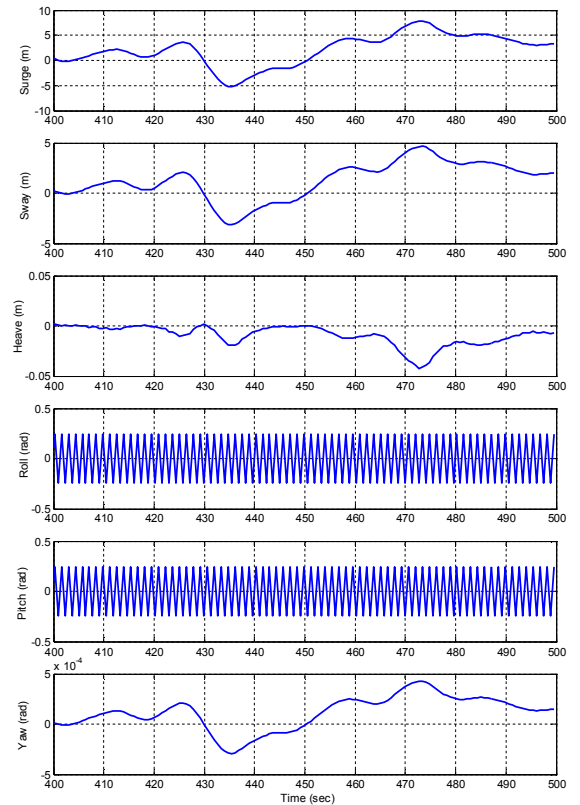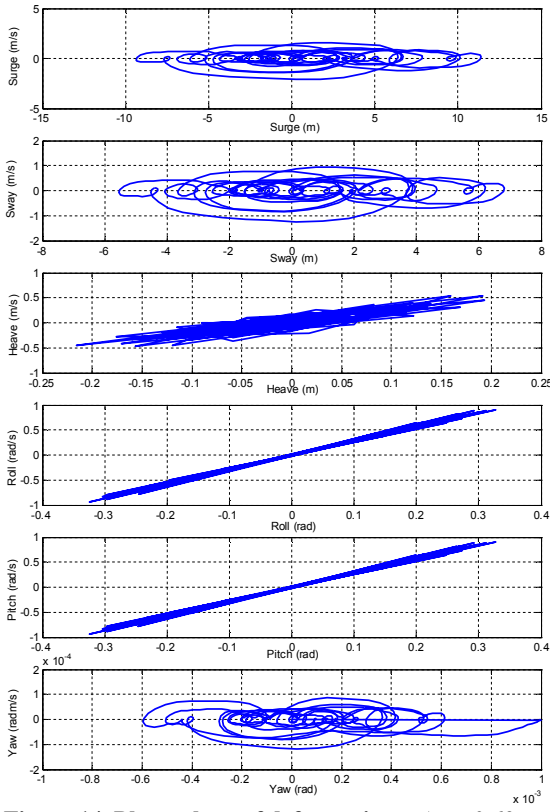
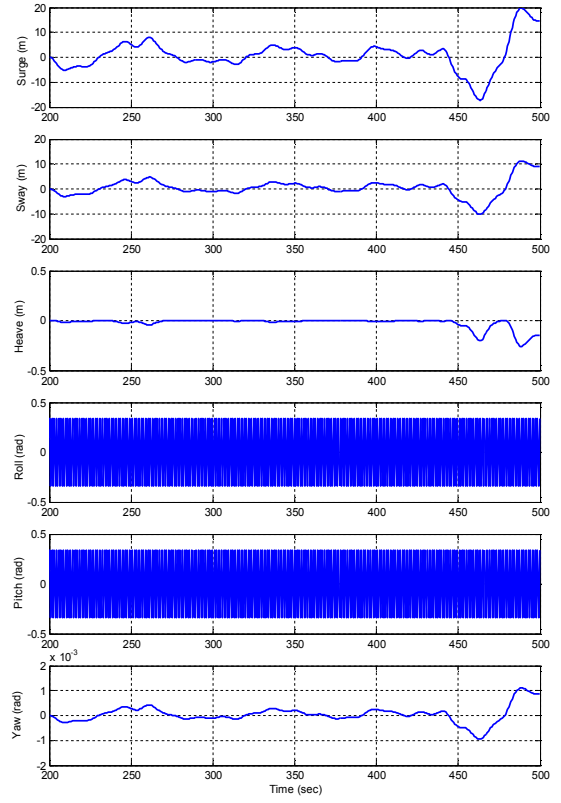**Figure 6. Phase plane of deformations,** $\Delta t = 0.67 \, \text{sec}$

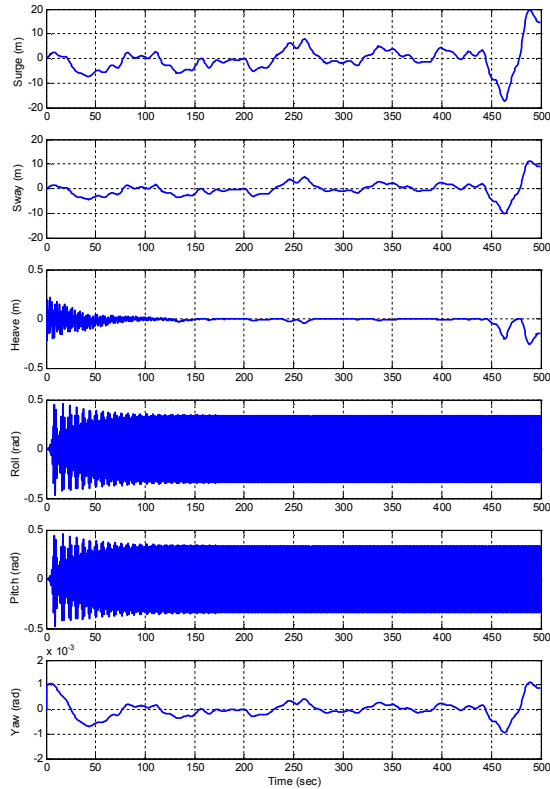**Figure 8. Time history of deformations in time between 200-500 sec,** $\Delta t = 0.68 \, \text{sec}$

Figure 7. Time history of deformations, $\Delta t = 0.68 \, \text{sec}$

Figure 9. Time history of deformations in time between 400-500 sec, $\Delta t = 0.68 \, \text{sec}$

Figure 10. Phase plane of deformations, $\Delta t = 0.68\,\text{sec}$

Figure 11. Time history of deformations, $\Delta t = 0.69\,\text{sec}$

Figure 12. Time history of deformations in time between 200-500 sec, $\Delta t = 0.69\,\text{sec}$
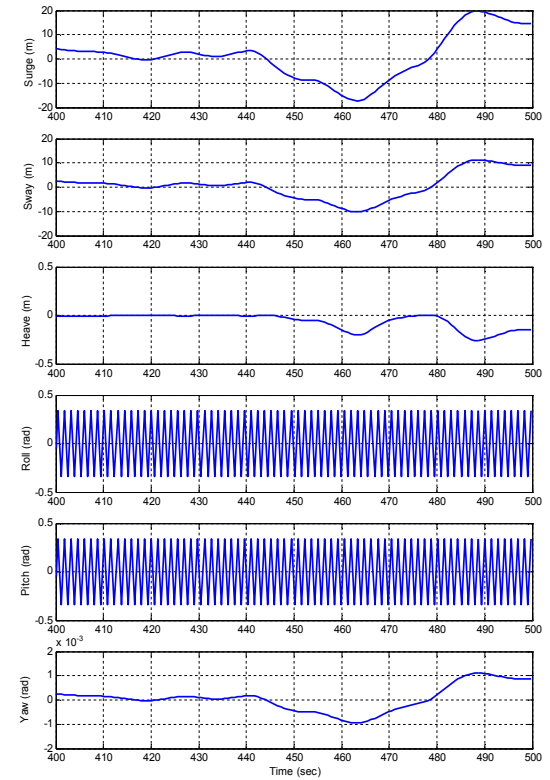

Figure 13. Time history of deformations in time between 400-500 sec, $\Delta t = 0.69\,\text{sec}$

Figure 14. Phase plane of deformations, $\Delta t = 0.69\,\mathrm{sec}$

Figure 16. Time history of deformations in time between 200-500 sec, $\Delta t = 0.7\,\mathrm{sec}$

Figure 15. Time history of deformations, $\Delta t = 0.7\,\mathrm{sec}$

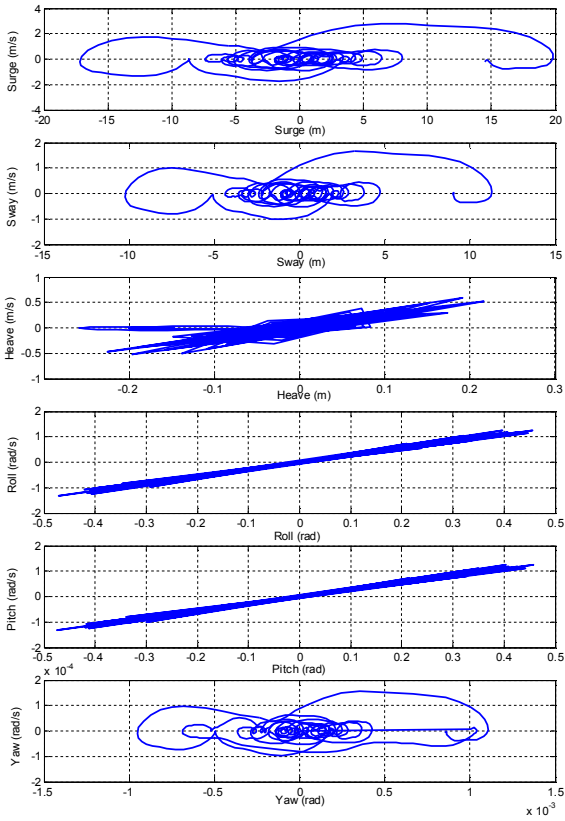**Figure 17. Time history of deformations in time between 400-500 sec, $\Delta t = 0.7\,\mathrm{sec}$**
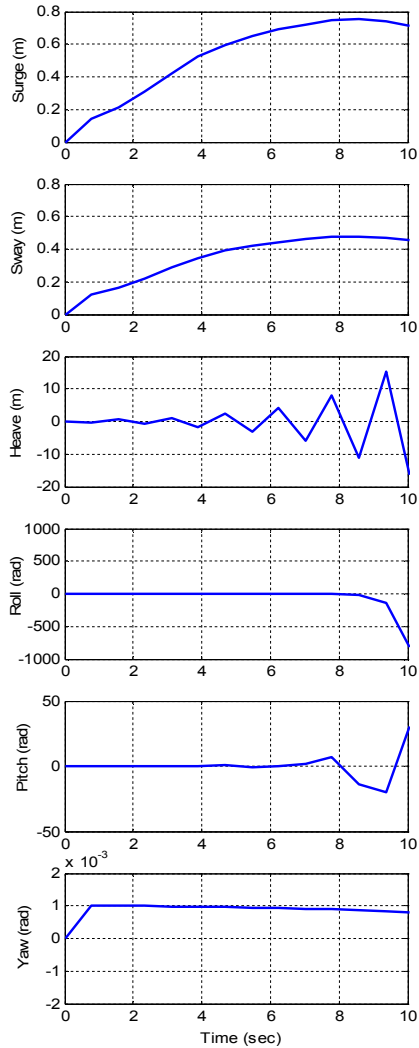
Figure 18. Phase plane of deformations, Δt=0.7sec

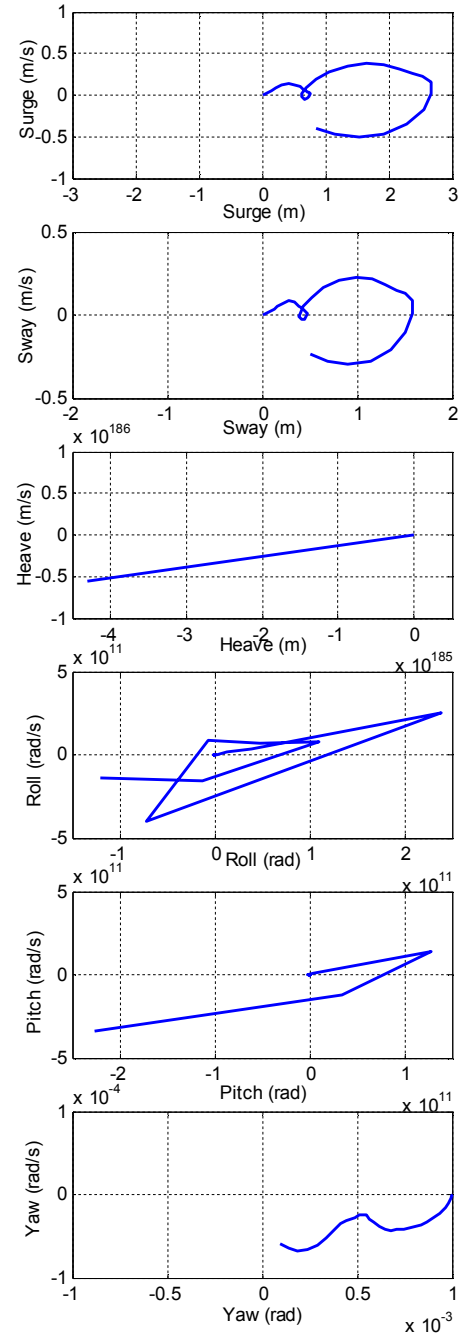

Figure 19. Time history of deformations sec, $\Delta t = 0.78$ sec

Figure 20. Phase plane of deformations, $\Delta t = 0.78$ sec